Appl. Phys. B 52, 14–21 (1991)

Applied Physics B Photophysics and Laser Chemistry

Generation of Excimer Emission in Dielectric Barrier Discharges

B. Gellert and U. Kogelschatz

Asea Brown Boveri, Corporate Research, CH-5405 Baden, Switzerland

Received 25 June 1990/Accepted 23 August 1990

Abstract. Dielectric barrier discharges (silent discharges) are used to excite a large number of excimers radiating in the VUV, UV or visible spectral range. The excited species include rare-gas dimers, halogen dimers as well as rare-gas halogen excimers and mercury halogen excimers. In many cases narrow-band UV radiation of typically 1–17 nm halfwidth and remarkable efficiency (1–10%) could be generated. Thus, dielectric barrier discharges provide a simple, versatile arrangement to study the basic reaction kinetics of excimer formation and also bear a substantial potential for large-scale industrial UV processes.

PACS: 52.80, 33.00, 82.50

Radiation sources emitting UV photons in the energy range of 5–10 eV have found a number of interesting applications because they are capable of splitting most chemical bonds. This has led to a number of new photo-initiated surface and volume processes like surface modification and cleaning as well as material deposition processes.

Many of these effects are being investigated with the aid of strong UV lasers, for example excimer lasers or nitrogen lasers. Alternatively, processes using UV lamps have been propagated. Due to their simplicity and reliability UV lamps have definite advantages over lasers when large-scale industrial processes are envisaged. Unfortunately, the available intensities especially in the vacuum UV range are very moderate. UV sources based on incoherent excimer emission [1–7] can provide an interesting alternative to conventional UV lamps.

The aim of this report is to demonstrate the potential of dielectric barrier discharges for excimer generation. We started out with the hypothesis that it should be possible to excite the excimers known from excimer lasers. In the course of the investigation it became apparent that the number of excimers that can be generated in these discharges is much larger. Their individual emission bands extend from the VUV to the visible part of the spectrum.

1. Dielectric Barrier Discharges

The dielectric barrier discharge is a very versatile high-pressure non-equilibrium discharge. Its electron energy lies in an ideal range for plasmachemical processes and can be controlled by external parameters. Today, the main application of the dielectric barrier discharge is the generation of ozone from air or oxygen. This process has become one of the major industrial plasmachemical syntheses [8]. The discharge configuration is characterized by the presence of at least one dielectric barrier in the current path between the electrodes and the discharge space. At higher pressure (0.1–10 bar) the discharge splits up into a large number of randomly distributed microdischarges of nanosecond duration. Each microdischarge consists of a thin cylindrical current filament which spreads into a surface discharge at the dielectric. The tiny plasma columns of the microdischarges can be characterized as high pressure transient glow discharges. Detailed experimental and theoretical investigations into the plasma parameters of these microdischarges were carried out with the aim of understanding and optimizing the performance of ozonizers [8–13]. The dielectric barrier serves two functions. It distributes the microdischarges evenly over the entire electrode area and it limits the amount of charge and energy that can be fed into an individual microdischarge. The duration of an individual microdischarge for a given gas is also determined by the dielectric barrier which provides the capacitive coupling to the external circuit. After typically a few nanoseconds a

microdischarge is choked due to charge build up on the dielectric which results in a local reduction of the electric field within the filament. Once the field falls below the ionization threshold, recombination and attachment processes take over and the current flow stops. Thus the current flow in a microdischarge is interrupted at a fairly early stage of discharge development. The plasma conditions in these microdischarges are ideal for excimer formation. The mean electron energy can be chosen to lie in the range of 1–20 eV and the electron density to be of the order 10^{14}–10^{15} cm^{-3}. The charge carriers are created in the microdischarges by direct impact ionization due to electrons accelerated in the imposed field. The mean energy of the electrons and the short duration of the microdischarges preclude noticeable heating of the heavy particles in the filaments and the surrounding gas. The major fraction of the energy gained by the electrons in the electric field is deposited in excited atomic and molecular states.

It is an important feature of these discharges that the plasma parameters can be influenced and thus optimised by external means. The mean electron energy is mainly controlled by the reduced electric field E/n at breakdown. This parameter can be influenced by the pressure in the discharge, the electrode spacing and the voltage slope dU/dt at breakdown. Figure 1 shows these relations for pure xenon [14]. In the left-hand part the dependence of the mean electron energy on the reduced electric field E/n is given. The right-hand part shows the relation between the reduced field at breakdown and the product of the particle density n times the gap spacing d. The lower curve corresponds to the Paschen curve which gives the criterion for stationary breakdown in a homogeneous field. With fast rising voltages and in configurations in which long time delays before breakdown are observed this Paschen condition can be overshot. In Fig. 1 the effective breakdown field was assumed to be 50% higher than the Paschen field. The arrows indicate the possibility of influencing the mean electron energy by changing the parameter nd. The electron density in a microdischarge can be controlled again by the pressure and by the properties of the dielectric barrier (thickness and dielectric constant).

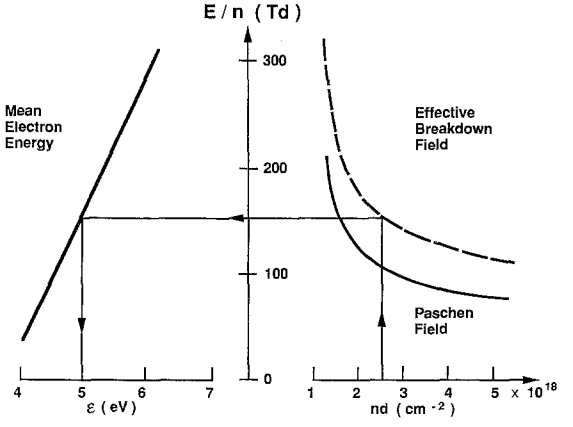

Fig. 1. Relation between mean energy ε of the electrons, reduced electric field E/n and the product of particle density n times gap spacing d for xenon

2. Experimental Arrangement

Utilizing the dielectric barrier discharge it is possible to construct UV sources of various geometries by making one or both electrodes and the dielectric barriers transparent to the radiation generated in the discharge space [4, 6]. Two experimental configurations were employed. The first configuration was used to study the emission in the spectral range above 150 nm. The geometry of such a cylindrical source of approximately 20 cm length is sketched in Fig. 2. In this case tubes of Suprasil 1 quartz were chosen as dielectric barriers, because of its dielectric properties and its superior UV transmission. The UV radiation was generated in an annular discharge gap containing different gas mixtures. The whole UV source was mounted in a thermostat that could be flooded with dry nitrogen and heated up to 150° C. The heating was achieved by applying heating wires around the outer surface of the thermostat. For investigations of iodide or bromide excimers a reservoir containing liquid bromine or solid iodine was attached to the source. The reservoir was connected by means of a valve to the source and was located outside the thermostat. This "cold spot" could be heated by a hot gas fan to generate a particular vapour pressure of iodine or bromine. Experiments with mixtures containing mercury were performed by filling a liquid drop of high-purity Hg into the annular discharge gap. With this configuration emission was detected that was emitted predominantly along the axis of the microdischarges. The second source was used to study radiation below 150 nm. In that case a construction made of glass was equipped with a LiF window through which the emission could be coupled out (Fig. 3b). The microdischarges always stand perpendicular to the dielectric and the electrodes. The configuration of Fig. 3b was constructed in such a way that the radiation emitted at 90 degree to the microdischarge axis was investigated.

Before filling the devices with high-purity gases they were cleaned chemically and by gas discharge sputtering and evacuated by a turbomolecular pump to pressures below 10^{-7} mbar. The discharges were driven by sinusoidal voltages in the frequency range between 50 Hz and several hundred kHz. Depending on gap spacing, gas composition and filling pressure the required peak voltages ranged from 3 to 20 kV. The charge transported across the gap and the voltage were registered by a fast transient digitiser. The electrical power was determined from a voltage versus charge Lissajous figure – a method

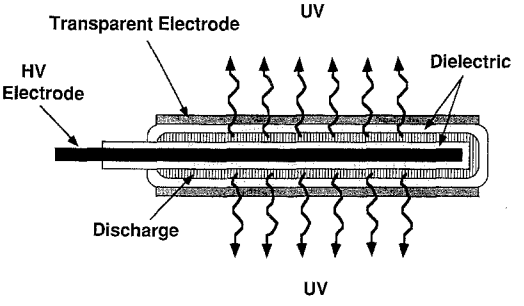

Fig. 2. Geometry of a cylindrical excimer source

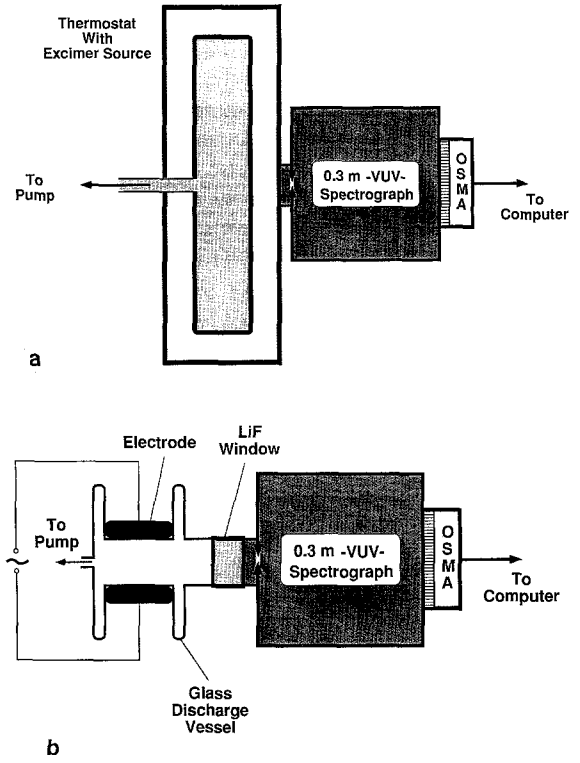

Fig. 3a, b. Experimental arrangement: **a** for measurements of spectra above 150 nm, **b** for measurements of spectra below 150 nm

that is well established for dielectric barrier discharges in ozone research [8].

Both devices could be connected to a 0.3 m VUV spectrograph (Acton Research, model VM 503). The complete arrangement as shown in Fig. 3a was flooded with dry nitrogen to overcome the absorption by air in the wavelength region below 200 nm. For the recording of UV spectra a VUV *o*ptical *s*pectrum *m*ulti channel *a*nalyzer (OSMA, Princeton Instruments, type IVUV 700) was mounted at the exit of the spectrograph. The local resolution in the spectral plane was better than 12 channels of the diode array per nm. The distance from one channel of the detector head to the next was 25 μm. The obtained spectra could be displayed and stored by a McIntosh II personal computer.

3. Results

3.1. Pure Rare-Gas Excimers

The first indication of molecular structures in spectra of helium discharges were found as early as 1913 [15, 16]. Extensive investigations into the properties of the He_2^* excimer were carried out by Hopfield [17] and the first mentioning of rare gas excimer formation in silent discharges was made by Tanaka [18]. The word excimer (**exci**ted di**mer**) is used to describe a slightly bound excited molecular state of complexes that do not possess a stable ground state. Apparently, all rare gases can form a slightly bound excited dimer lying about 8–20 eV above the repulsive ground state and having a potential dip of about 0.5–2 eV. In our discharges rare-gas (Rg) excimer formation involves mainly two steps: The excitation of a rare gas atom Rg by electrons of suitable energy and the formation of the excimer complex by a three body reaction.

$$e + Rg \rightarrow e + Rg^*, \quad (1)$$

$$Rg^* + Rg + Rg \rightarrow Rg_2^* + Rg. \quad (2)$$

The first step requires an electron energy of at least 8–20 eV. The second step occurs only if reaction (2) is faster than any de-excitation processes of Rg* like radiative transitions or collisional quenching. In addition, the Rg_2^* complex is initially formed in a vibrationally excited state which has to be stabilized before it can fall apart. Since step (2) is a three body reaction a higher pressure will always favour excimer formation.

In addition to this straight forward reaction, additional reaction paths involving higher lying excited states and electronic recombination processes of Rg^+ and Rg_2^+ have to be considered. In electro-negative gases also the recombination of positive and negative ions can be a major path leading to excimer formation.

Detailed calculations treating Xe_2^* formation in dielectric barrier discharges in pure xenon were presented in [6]. The electron energy distribution function was obtained by solving the Boltzmann equation for a weakly ionized xenon plasma. A fairly complex reaction scheme treated reactions involving electrons and charged and excited atomic and molecular xenon species. The predicted intrinsic UV efficiency under optimum discharge conditions reaches about 40%. This high value is in agreement with recent calculations performed for electron beam excitation of xenon [19] and krypton [20]. The best experimental UV efficiencies for xenon in the dielectric barrier discharge are close to 10% [6]. Considering the solid angle of the detection system and the transmission of the quartz envelope this value would correspond to an intrinsic efficiency of about 30%.

For efficient excimer formation certain conditions have to be fulfilled. The two main requirements of a reasonably elevated electron energy and simultaneously a high gas pressure require a high-pressure non-equilibrium discharge. Since no common stationary discharge can fulfil these requirements a repetitively pulsed discharge like the silent discharge with its many microdischarges is ideally suited for this purpose.

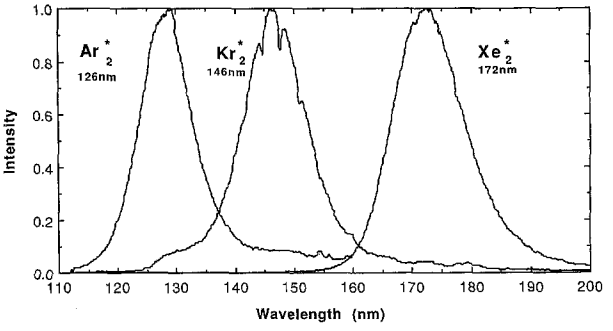

Fig. 4. Spectra of Ar_2^*, Kr_2^*, Xe_2^* excimers in a dielectric barrier discharge

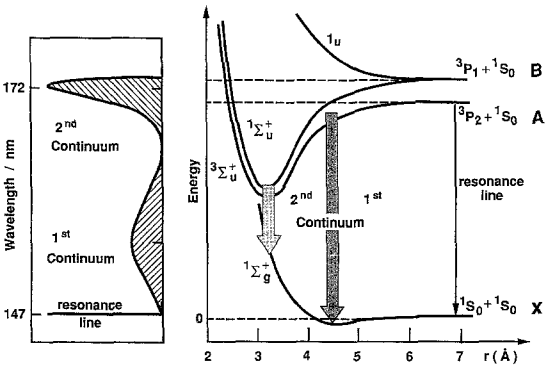

Fig. 5. Part of the potential energy diagram of xenon and corresponding excimer emission (after [21])

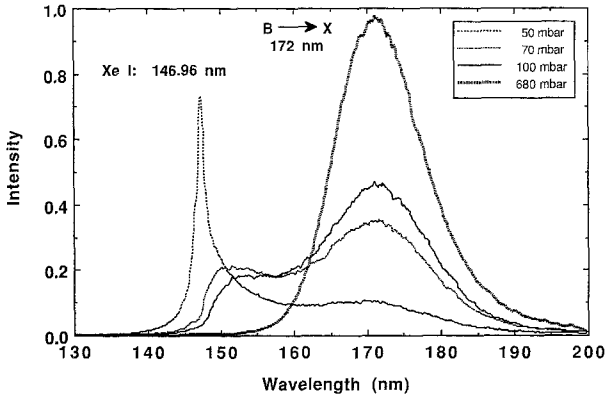

Fig. 6. Pressure dependence of the xenon spectrum in a dielectric barrier discharge. At low pressure a homogeneous glow discharge is established radiating mainly at the resonance line. Increasing pressure leads to more and more excimer radiation and a visible transition to the fully established microdischarge mode

Our investigations were restricted to wavelengths above 100 nm. For this reason we only recorded the excimer continua of argon, krypton, and xenon. Figure 4 shows the intense second continua which correspond to a transition from the lowest vibrational levels of the two lowest lying bound electronic excimer levels ($^1\Sigma_u^+$, $^3\Sigma_u^+$) to the repulsive ground state. The half width of these continua is about 10–17 nm.

Taking xenon as an example we can clearly show the transition from the resonance line at 147 nm to the first continuum at 150 nm and finally to the second continuum at about 170 nm with rising pressure (Figs. 5, 6). The resonance line dominating at 50 mbar results from a transition $^3P_1 - {}^1S_0$, the first continuum appearing at 100 mbar corresponds to transitions from vibrationally excited excimer states ($^1\Sigma_u^+$, $^3\Sigma_u^+$) to the shallow minimum of the ground state potential resulting in emission around 150 nm [21, 22]. At higher pressure clearly the second continuum at 170 nm dominates.

The change of the emission characteristics from resonance line to first and second continuum correlates with a visible change of discharge modes. At low pressure the discharge appears to be a homogeneously radiating glow discharge. In the medium pressure range tiny microdischarges are superimposed on a continuous background. Towards the high-pressure end very many bright microdischarges dominate. There are even gas mixtures and discharge conditions where the homogeneous background radiation disappears completely. For fixed gap spacing the transition between the various modes depends on the gas mixture, pressure and excitation frequency of the discharge. The following investigations deal mainly with the fully established microdischarge mode.

3.2. Halogen Dimers

In the past, spectra of halogen dimers were investigated, in particular, to understand the excimer formation that was exploited in excimer lasers. There are detailed investigations for Br_2, I_2 by Tellinghuisen [23, 24] and for F_2 and Cl_2 e.g. by Diegelmann et al. [25] and Castex et al. [26]. The studies aimed at exact identification of the electronic states that are responsible for a possible laser emission. Figure 7 shows the corresponding potential energy curves of a homo-nuclear halogen molecule after [23]. According to Mullikan's [27] qualitative studies these excited states are bound. For Br_2 and I_2 it was demonstrated in [23, 24] that the band systems at 289 and 342 nm are due to a $D'(^3\Pi_{2g}) - A'(^3\Pi_{2u})$-transition. According to Diegelmann [25] the same is to be expected for F_2^* and Cl_2^* with the band systems at 158 and 259 nm.

By means of the arrangement depicted in Fig. 3a experiments were performed with mixtures of about 2% F_2 in He and about 5% Cl_2 in Ar at a total pressure of 400–800 mbar. Strong F_2^* and Cl_2^* emission was found without special efforts. A well structured modulation could be observed. The spacing of the relative maxima of the spectra was approximately 0.8 nm for F_2^* and 1.2 nm for Cl_2^* which is very similar to that observed and interpreted by Diegelmann et al. in experiments with pulsed e-beam (Febetron) excitation [25]. To excite Br_2

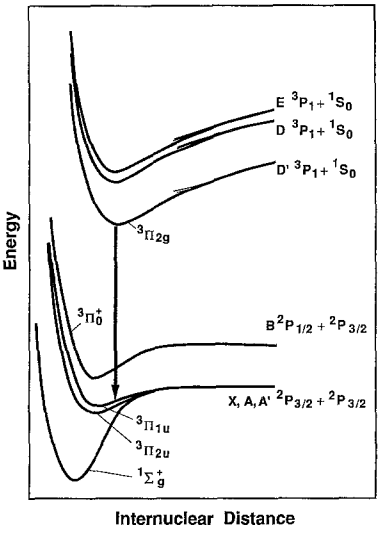

Fig. 7. Part of the potential energy diagram of halogen molecules and principal excimer transition (after [24])

and I_2, vapour of bromine or iodine was transmitted into the device that was filled by 500 mbar of Ar. The Br pressure was in the range of 0.9 bar whereas the iodine pressure was approximately 10^{-2} bar. Again, we succeeded in obtaining Br_2^* and I_2^* emission. The modulation was between 0.8 and 1.2 nm for the Br_2^* emission and around 1.5 nm for I_2^*. Figure 8 gives an overview of the obtained halogen dimer spectra.

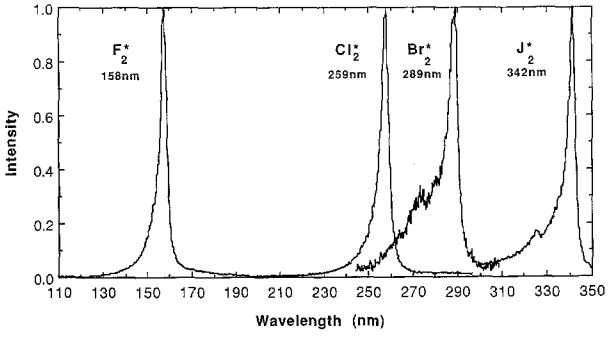

Fig. 8. Spectra of F_2^*, Cl_2^*, Br_2^*, I_2^* excimers in a dielectric barrier discharge

3.3. *Rare-Gas Halogen Excimers*

Rare-gas halogen excimers are amongst the most extensively investigated excimers, because their transitions are used in commercial lasers. Review articles can be found e.g. in [28–30]. Part of a typical energy diagram is sketched in Fig. 9.

The ground state (labelled X) is always repulsive, whereas the excited states are bound. Because of the spin-orbit splitting of the halogen atom the ground state is of complicated structure. In general, the van der Waal's minimum is comparable to kT (e.g., 255 cm^{-1} for XeCl). For the fluorides it is much larger (e.g., 1065 cm^{-1} for XeF, see, e.g., the paper by Brau in [28]). The first excited bound states are of ionic type, since they are generated by a positive rare gas ion ^2P Rg^+ and a negative halogen ion ^1S X^-(X = F, Cl, Br, I). Due to spin-orbit splitting for halogens of high atomic number there are two nearly

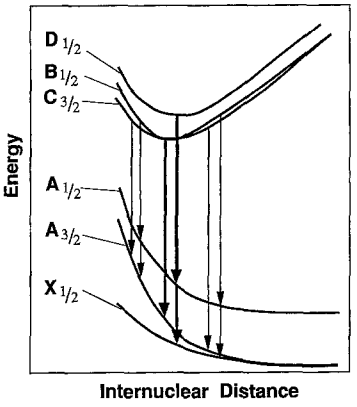

Fig. 9. Part of the potential energy diagram of rare gas halogen molecules and corresponding excimer transitions demonstrated with ArBr (after [33])

adjacent states of that kind. The lower state from the rare-gas ion of the level $^3P_{3/2}$ (Rg^+) is spin-orbit split into $^2\Pi_{3/2}$ and $^2\Sigma_{1/2}$. The upper is a $^2\Pi_{1/2}$ state, coming from the $^2P_{1/2}$ (Rg^+) level of the rare-gas ion. These states are labelled *B*, *C*, *D*. For some molecules the *B* state is of higher energy than the *C* state. The typical strong laser transitions are *B–X* transitions. The *B–X* and *D–X* transitions have the highest transition moments and show the strongest fluorescence. The *C–A* transition is weaker and leads to broad band emission (strongly repulsive part of the ground state). The various physical mechanisms that contribute to excimer generation are discussed, e.g., in [31], for experiments with synchrotron radiation. Detailed theoretical modelling of rare gas halogen excimer generation in dielectric barrier discharges can be performed similar to the modelling of Xe_2^* formation [6] and will be reported in a separate paper.

The distribution of the vibronic levels of a particular state and also the distribution of the population between the *B*, *C*, and *D* states depend on the donator (binding energy of the various possible gases), the precursor (rare-gas or halogen excitation, i.e. excited atom or molecule or corresponding ions) and on the energy distribution of the components of the discharge. E.g., the well investigated dependence of the vibronic state distribution on pressure has in that way been explained [32]. It is the special advantage of the dielectric barrier discharge that the electron energy distribution can be influenced over a wide range by simple means, e.g. by variation of the buffer gas pressure. Due to that property optimized and efficient excimer formation is possible for – as we think – probably every excimer known today. Because of that feature also influencing of the spectral shape of the excimer emission, e.g., variation of the halfwidth or changing of relative intensities of different emission bands can be achieved.

Chloride, fluoride, bromide and iodide excimers were generated with the arrangement of Fig. 3a. Figure 10a shows an overview of the obtained chloride excimer spectra. A mixture of 5% Cl_2 in Ar or He was used and mixed with Ar, Kr, or Xe of high purity. The total pressure was between 100 and 900 mbar. Shape and width of the *B–X* emission can be varied by pressure variation. Full width half maximum at 120 mbar of total pressure was found to be 6.6 nm for XeCl* decreasing to approximately 2 nm at 920 mbar [33]. At the same time the UV efficiency (UV output at 308 nm divided by the electrical input into the discharge) increased to more than 12%. Cl_2 fluorescence at 259 nm diminishes for pressures in excess of approximately 400 mbar. The *C–A* emission is weak at low pressure and increases up to approximately 400 mbar. The *D–X* emission declines with rising pressure. While it was found in experiments with excitation by synchrotron radiation that the Cl_2^* fluorescence at 259 nm is of comparable magnitude as the fluorescence from ArCl* [31], this is not the case in the experiments conducted in this study. In the silent discharge at pressures above 200 mbar ArCl* emission at 175 nm dominates by far.

In addition to XeCl*, the rare-gas fluorides belong to the most common excimer laser media. Because of the corrosive properties of fluorine special materials had to be used in the gas handling and mixing system. The observed

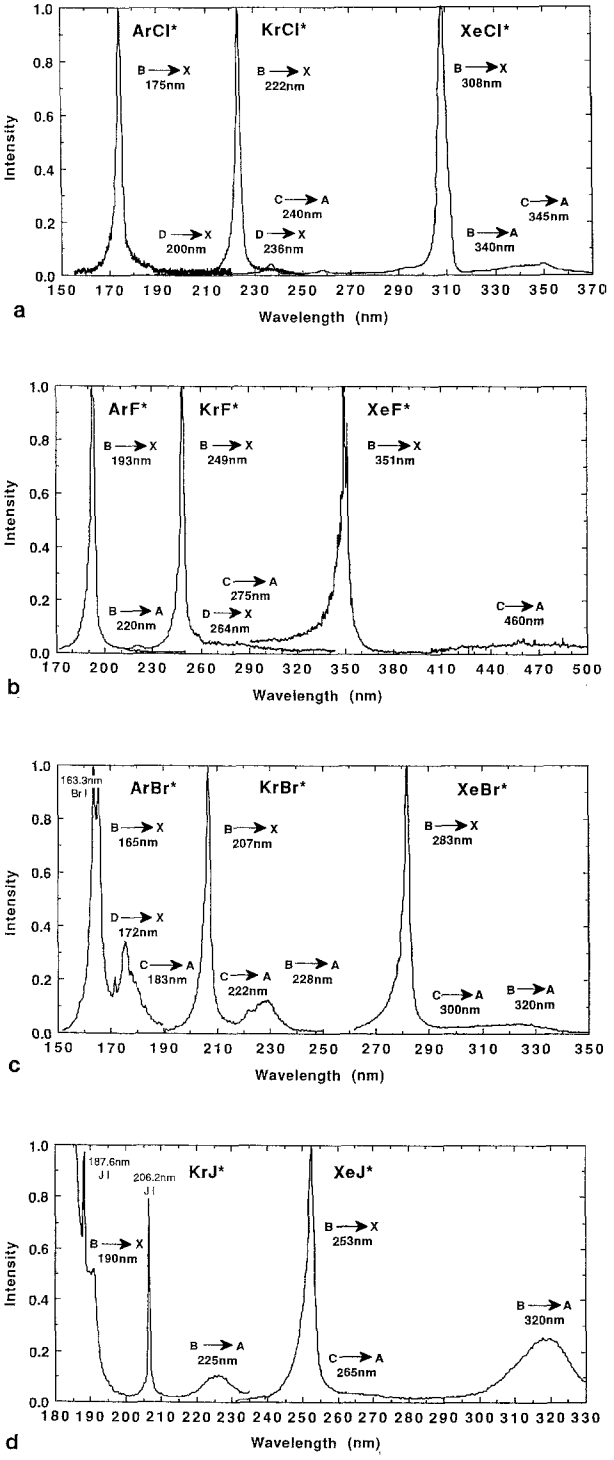

Fig. 10a–d. Spectra of rare gas halogenide excimers in a dielectric barrier discharge: **a** chlorides, **b** fluorides, **c** bromides, **d** iodides

halfwidths of the *B–X* transitions at 900 mbar total pressure ranged from 2.8 nm (ArF*) to 4 nm XeF*. For KrF* also the *B–A* and *C–A* transitions and for XeF* also the *D–X* and *C–A* transitions could be identified, as shown in Fig. 10b.

The generation of bromide excimers was most efficient for Xe and least efficient for Ar. The UV efficiency for XeBr was estimated to be close to 10%. As Fig. 10c demonstrates, the *B–X* transitions are strongest. The halfwidth of the *B–X* transitions is about 2 nm at the pressure used. The figure gives spectra that were obtained in silent discharges at approximately 1 bar total pressure. Detailed studies have been performed by Tamagake et al. [34] for the XeBr* molecule, where e.g. a *B/C* ratio of 1.5 was found for low pressure. Approximately the same ratio could be found in the dielectric barrier discharge. The ratio increases with pressure due to collisional transfer from *C* to *B*. Whereas the identification of the *C–A* and *B–A* transitions is clear for XeBr and KrBr, the *D–X* transition of ArBr is doubtful, because under the conditions of the experiment atomic lines are superposed. A discussion of the special ArBr* spectrum, potential energy curves and effects influencing the spectrum can be found in [35]. A typical example is the strong BrI emission at 163.3 nm. For ArBr the ionic state barely crosses the lowest covalent state correlating to an excited halogen atom and the ionic state may predissociate [36, 37]. This may be the reason why only weak emission could be observed. Similarly, as observed by Tellinghuisen in experiments with Tesla discharges [38], spectra of the *B–X* and *B–A* transitions are of larger halfwidth at low pressure, where the excited vibrational levels make greater relative contributions to the total emission. Excimers in mixtures of iodine and rare gases could be obtained for krypton and xenon. Iodide excimer emission was weaker than excimer emission with other halogens. The reason for this effect could be that only low iodine pressures were used (10^{-2} bar) or that quenching especially for the higher excited states is of greater importance. The spectra of Fig. 10d were obtained for a total pressure of 500 mbar. Apart from the narrow *B–X* transition (2 nm halfwidth) also the wide *B–A* transition (20 nm halfwidth) is rather strong. With increasing pressure the *B–X* transition dominates. Because of the same arguments given for the ArBr* emission also KrI* emission is difficult to obtain and weak in intensity. Clearly, atomic iodine lines are superposed (e.g., JI 206.2 nm, JI 187.6 nm). Further strong iodine lines can be found below 185 nm. A more detailed discussion of the rare gases iodide spectra can be found in [34, 39].

3.4. Mercury-Vapour Excimers

A strong similarity of the mercury-halogen molecules with the rare-gas halogen systems is immediately apparent from a comparison of the corresponding potential curves (see, e.g., Gallagher in [28]). This reflects the fact that the Hg atom behaves very much like a rare-gas atom. The relatively weakly bound ground states and strongly bound ionic states, as shown for the rare-gas halogen excimers in Fig. 9 can be found again. So nearly the same type of transitions can be expected. On the other hand, since the lowest excited states of Hg occur at an energy considerably below that of the rare-gas excited levels, the mercury halides radiate at longer wavelengths in the visible part of the spectrum. Correspondingly the radiative lifetimes are longer for mercury halides. For those molecules containing a heavy halogen, e.g., HgBr* or HgI* spin orbit coupling is strong. Laser action could be

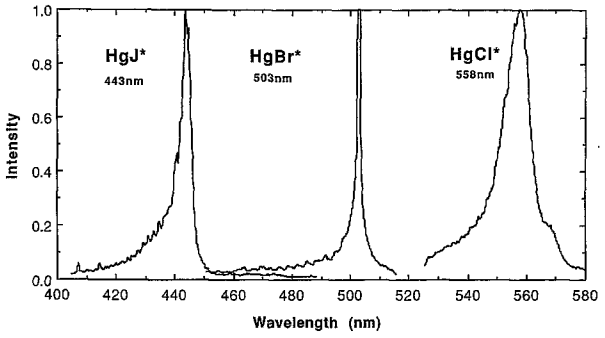

Fig. 11. Spectra of mercury halogen excimers in a dielectric barrier discharge

obtained on the B–X transition of the HgX (X = Cl, Br, I) radical by electron beam excitation, photodissociation of HgX_2 molecules or avalanche discharge pumping (for a list of references see, e.g., [40]). Work is under way to develop a mixed mercury halide laser with a multicomponent output spectrum [40, 41].

For spectroscopic studies Hg halides have been produced in many ways, e.g., in experiments using pulsed electron beam excitation (Febetron) by heating the stable dihalides thus producing sufficient vapour pressure [43] or even in dielectric barrier discharges of special geometry [44]. Malinin et al. [44] used 30–40 kV pulses of 50 ns duration to excite mixtures of Hg, Br_2, CCl_4, $CHCl_3$ and rare gases. The pressure of the discharge was up to 1 bar. Contrary to the experiments reported here the researchers claimed to have obtained a rather homogeneous discharge. This might be due to the special geometry, electrical and discharge conditions that were employed. HgCl* and HgBr* emission was found to be close to the threshold of laser action.

The mercury halogen excimer spectra from dielectric barrier discharges shown in Fig. 11 were obtained by heating the discharge device to temperatures around 75° C. Approximately 500 mbar of Ar was used as a buffer gas. For the excitation of HgCl* a mixture of 5% Cl_2 in Ar was used. The halfwidth of HgBr* is surprisingly small (1.6 nm), whereas for HgI* it is 4.2 nm and rather broad for HgCl* (10 nm). Possibly, this might be due to different halogen contents in the discharge. At low pressure also the $D-X$ transitions were observed with higher strength. A general discussion of the spectra of the Hg halides in the wavelength range from 300 to 580 nm can be found in [40].

Due to its low-lying energy states mercury is also very well suited for the generation of mercury rare gas excimers as, e.g., HgXe* which radiate in the UV to VUV wavelength range. Because of the special nature of this emission a more detailed report is published elsewhere [45].

4. Discussion

So far most investigations into excimer formation used complicated and expensive sources like energetic particle beams or synchrotron radiation. We have demonstrated that a large number of different excimers can be generated in a rather simple gas discharge with a dielectric barrier. It is possible to excite excimers radiating in VUV, UV or even in the visible spectral range. UV efficiencies of these sources are of the order of 1–10%. The spectral behaviour of excimer radiation from dielectric barrier discharges is very similar to that found by other excitation techniques. Basic spectroscopic investigations can therefore be performed with these sources as well.

The transition from the well known glow discharge at low pressure ($\leqq$ 50 mbar) to the fully established high pressure dielectric barrier discharge is accompanied by a visible transition from a homogeneously radiating glow discharge mode to the discrete microdischarge mode. In that case the radiation is produced within many tiny current filaments in the gap between the dielectrics. With the change of the discharge modes the radiation shifts from resonance line emission to the broader excimer band emission. Because of its special property that the mean electron energy can be influenced by external means, the dielectric barrier discharge is an ideal tool to study reactions leading to excimer formation and optimise the plasma parameters. In many cases the reaction kinetics leading to the formation of a special excimer complex is extremely selective. It is thus possible to construct radiation sources with high intensity in certain narrow spectral regions.

There are a number of UV induced industrial photochemical and photophysical processes that require intense radiation in certain well defined spectral regions. The photolytic deposition of metal, dielectric or semiconductor layers is a new and important application [14, 46]. In addition, photochemical syntheses, polymerization and degradation processes are under investigation. The dielectric barrier discharge configuration is also very flexible with respect to geometry which helps in irradiating large volumes or curved surfaces. Its capability of industrial upscaling has been demonstrated in large ozone generators reaching megawatt power levels. The combination of the dielectric barrier discharge with the most striking property of the excimers, namely the absence of a stable ground state, opens up the possibility of designing a new generation of intense UV and VUV sources which do not suffer from the limitations of radiation trapping.

References

1. A.K. Shuaibov, V.S. Shevera: Sov. Phys. Tech. Phys. **24**, 976 (1979) and **25**, 434 (1980)
2. G.A. Volkova, N.N. Kirillova, E.N. Pavslovskaya, A.V. Yakovleva: J. Appl. Spectrosc. **41**, 1194 (1984)
3. X. Xu: Proc. 8th Int'l Conf. on Gas Discharges & Their Applications, Oxford (1985), p. 580
4. B. Eliasson, U. Kogelschatz, H.J. Stein: Europ. Photochem. Ass. Newslett. **32**, 29 (1988)
5. V.V. Kapustin, I.G. Rudoi, A.M. Sorokova: Sov. J. Plasma Phys. **14**, 808 (1988)
6. B. Eliasson, U. Kogelschatz: Appl. Phys. B **46**, 299 (1988)
7. H. Kumagai, M. Obara: Appl. Phys. Lett. **54**, 2619 (1989)
8. U. Kogelschatz: in: *Process Technologies for Water Treatment*, ed. by S. Stucki (Plenum, New York 1988) pp. 87–120
9. V.I. Gibalov, V.G. Samoilovich, Y.V. Philippov: Russ. J. Phys. Chem. **55**, 471 (1981)

10. C. Heuser: Zur Ozonerzeugung in elektrischen Gasentladungen. Dissertation, RWTH Aachen (1985)
11. B. Eliasson, M. Hirth, U. Kogelschatz: J. Phys. D **20**, 1421 (1987)
12. R. Peyrous, P. Pignolet, B. Held: J. Phys. D **22**, 1658 (1989)
13. K. Yoshida, H. Tagashira: Tech. Meet. on Electrical Discharges, Hakone (1987) Paper No. ED-87-56, IEE of Japan
14. U. Kogelschatz: Invited Plenary Lecture, 9th Int. Symp. on Plasma Chemistry, Pugnochiuso, Italy (1989) Pure and Appl. Chem. **62**, 1667 (1990)
15. F. Goldstein: Verh. Deutsch. Phys. Ges. **15**, 402 (1913)
16. W.E. Curtis: Proc. Roy. Soc. London A **89**, 146 (1913)
17. J.J. Hopfield: Astrophys. J. **72**, 133 (1930)
18. Y. Tanaka: J. Opt. Soc. Am. **45**, 710 (1955)
19. D.J. Eckstrom, H.H. Nakano, D.C. Lorents, T. Rothem, J.A. Betts, M.E. Lainhart, D.A. Dakin, J.E. Maenchen: J. Appl. Phys. **64**, 1679 (1988)
20. D.J. Eckstrom, H.H. Nakone, D.C. Lorents, T. Rothem, J.A. Betts, M.E. Lainhart, K.J. Triebes, D.A. Dakin: J. Appl. Phys. **64**, 1691 (1988)
21. D. Haaks: *Kinetik der* Xe_2^*- *und* Kr_2^*-*Excimere.* Habilitationsschrift, University of Wuppertal (1980)
22. A. Ulrich, B. Busch, W. Krötz, J. Wieser, D.E. Murmick: Proc. 7th Int'l Conf. on High Power Particle Beams, Karlsruhe (1988) 1, p. 736
23. J.B. Tellinghuisen: Chem. Phys. Lett. **49**, 485 (1977)
24. J.B. Tellinghuisen: In *High Power Laser and Applications*, ed. by K.L. Kompa, H. Walther, Springer Ser. Opt. Sci. **9** (Springer, Berlin, Heidelberg 1987) p. 110
25. M. Diegelmann, H. Hohla, F. Rebentrost, K.L. Kompa: J. Chem. Phys. **76**, 1233 (1982), M. Diegelmann: PLF-Report no. 33 (Aug. 1980), Max-Planck-Inst., Projektgruppe Laserforschung, D-8046 Garching bei München
26. J. LeCalvé, M.C. Castex, D. Haaks, B. Jordan, G. Zimmerer: Nuov. Cim. **63** (B), 265 (1981)
27. R.S. Mullikan: J. Chem. Phys. **55**, 228 (1971)
28. C.K. Rhodes (ed.): *Excimer Lasers*, 2nd edn., Topics Appl. Phys. **30** (Springer, Berlin, Heidelberg 1984)
29. K.L. Kompa, H. Walther (eds.): *High Power Lasers and Applications*, Springer Ser. Opt. Sci. **9** (Springer, Berlin, Heidelberg 1987)
30. I.S. Lakoba, S.I. Yakovlenko: Sov. J. Quantum Electron. **10**, 389 (1980)
31. B. Jordan: Dissertation, Department of Physics, University of Hamburg (1983)
32. T.D. Dreiling, D.W. Setser: J. Chem. Phys. **75**, 1360 (1981)
33. B. Gellert, B. Eliasson, U. Kogelschatz: Proc. 5th Int'l Symp. on the Science Technology of Light Sources LS5, York (1989), p. 155
34. K. Tamagake, D.W. Setser, J.H. Kolts: J. Chem. Phys. **74**, 4286 (1981)
35. M.F. Golde, A. Kvaran: J. Chem. Phys. **72**, 434 and 442 (1980)
36. J.J. Ewing, C.A. Brau: Phys. Rev. A **12**, 129 (1975)
37. C.A. Brau, J.J. Ewing: J. Chem. Phys. **63**, 4640 (1975)
38. J. Tellinghuisen, M.R. McKeever: Chem. Phys. Lett. **72**, 94 (1980)
39. M.P. Casassa, M.F. Golde, A. Kvaran: Chem. Phys. Lett. **39**, 51 (1978)
40. A.J. Berry, C. Whitehurst, T.A. King: J. Phys. D **21**, 39 (1988)
41. C. Whitehurst, T.A. King: J. Phys. D **20**, 4035 and 4053 (1987)
42. S.P. Bazulin, N.G. Basov, S.N. Bugrimov, V.S. Zuev, A.S. Kamrukov, G.N. Kashnikov, N.P. Kozlov, P.A. Ovnichinnikov, A.G. Opekan, Yu.S. Protasov: Sov. J. Quantum Electron. **16**, 663, 836 and 990 (1986)
43. R.W. Waynant, J.G. Eden: Appl. Phys. Lett. **33**, 708 (1978)
44. A.N. Malinin, A.K. Shuaibov, V.S. Shevera: J. Appl. Spectrosc. **32**, 313 (1980)
45. B. Eliasson, B. Gellert: J. Appl. Phys. **68**, 2026 (1990)
46. H. Esrom, J. Demny, U. Kogelschatz: Chemtronics **4**, 202 (1989)